unclassified

SECURITY CLASSIFICATION OF THIS PAGE (When Data Entered)

REPORT DOCUMENTATION PAGE		READ INSTRUCTIONS BEFORE COMPLETING FORM
1. REPORT NUMBER SAIC-84-1429/PRI-87	2. GOVT ACCESSION NO.	3. RECIPIENT'S CATALOG NUMBER
4. TITLE (and Subtitle) Final Report for the Contract on "Conversion Efficiencies of Charged Particle Beam Driven Free Electron Lasers"		5. TYPE OF REPORT & PERIOD COVERED Final Report 6/11/79 - 11/30/84 6. PERFORMING ORG. REPORT NUMBER
7. AUTHOR(s) R. E. Aamodt, R. C. Davidson, G. L. Francis, B. Hafizi, and K. T. Tsang		8. CONTRACT OR GRANT NUMBER(s) N00014-79-C-0555
9. PERFORMING ORGANIZATION NAME AND ADDRESS Science Applications International Corp. Plasma Research Institute, 934 Pearl Street, Boulder, Colorado 80302		10. PROGRAM ELEMENT, PROJECT, TASK AREA & WORK UNIT NUMBERS 61153N RR011-07-03 NR 020-044
11. CONTROLLING OFFICE NAME AND ADDRESS Office of Naval Research Physics Division Office (Code 412) 800 N. Quincy St., Arlington, VA 22217		12. REPORT DATE November 29, 1984 13. NUMBER OF PAGES 28
14. MONITORING AGENCY NAME & ADDRESS (if different from Controlling Office)		15. SECURITY CLASS. (of this report) unclassified 15a. DECLASSIFICATION/DOWNGRADING SCHEDULE

16. DISTRIBUTION STATEMENT (of this Report)

Approved for public release; distribution unlimited.

17. DISTRIBUTION STATEMENT (of the abstract entered in Block 20, if different from Report)

18. SUPPLEMENTARY NOTES

19. KEY WORDS (Continue on reverse side if necessary and identify by block number)

free electron lasers

20. ABSTRACT (Continue on reverse side if necessary and identify by block number)

see reverse

DD FORM 1473, 1 JAN 73 EDITION OF 1 NOV 65 IS OBSOLETE
S/N 0102-LF-014-6601

unclassified

SECURITY CLASSIFICATION OF THIS PAGE (When Data Entered)

Abstract. block # 20

This report constitutes the final report of research with ONR under contract no. N00014-79-C-0555, and entitled "Conversion Efficiencies of Charged Particle Beam Driven Free Electron Lasers".

The contract covered the period from June 11, 1979 to November 30, 1984. Technical progress herein reported covers this entire period; however, in depth technical details specialize in the final year as other annual reports have thoroughly reviewed the work of previous years. Additionally, the totality of publications and talks resulting directly from this contract over the entire contract period are listed.

SAIC-84/1429
PRI-87

November 29, 1984

Final Report
for the Contract on
"Conversion Efficiencies of Charged Particle Beam Driven Free Electron Lasers"

by

R. E. Aamodt, R. C. Davidson,* G. L. Francis,
B. Hafizi, and K. T. Tsang

Science Applications International Corporation
Plasma Research Institute
934 Pearl Street
Boulder, Colorado 80302

Research supported by the Office of Naval Research
under Contract No. N00014-79-C-0555

*Permanent address: Plasma Fusion Center, Massachusetts Institute of Technology, Cambridge, Massachusetts 02139

ABSTRACT

This report constitutes the final report of research with ONR under contract no. N00014-79-C-0555, and entitled "Conversion Efficiencies of Charged Particle Beam Driven Free Electron Lasers".

The contract covered the period from June 11, 1979 to November 30, 1984. Technical progress herein reported covers this entire period; however, in depth technical details specialize in the final year as other annual reports have thoroughly reviewed the work of previous years. Additionally, the totality of publications and talks resulting directly from this contract over the entire contract period are listed.

I. INTRODUCTION

The general purpose of the research under this contract was to develop sophisticated models of electron beam driven free electron lasers in order to more accurately predict radiation gain rates and fundamental efficiencies. Over the period covered by the contract a number of magnetic field and beam configurations were studied but primary emphasis has been on helical, longitudinal, and planar wigglers with strong guide fields.

Within this area low energy, high current devices were studied the most, aiming at an understanding of high gain, long pulse devices. Such systems usually formulate the analytic amplification problem by choosing beam equilibrium and linearly perturbing about it to calculate (linear) gain rates, and then the nonlinear saturation mechanisms are studied separately in order to evaluate the leading limiting mechanism. Again such analyses dominated our research program and these results are discussed in the following sections, previous progress reports, and our total publications. Additionally, part of our studies analyzed the all-important question of the existence of an equilibrium about which to perturb and significantly it was found that the properly posed problem of a beam with finite emittance being emitted from a diode does not always give a satisfactory equilibrium type solution. This example has pointed out the need for more careful analyses of the so-called equilibrium problem. As FEL gain rates tend to be sensitively dependent on the shape of the velocity space distribution functions and nonlinear saturation depends on the three dimensional nature of the amplified wave, wiggler, and beam distribution function a properly chosen set of beam propagation features must be carefully determined. Most probably this will require a very strong coupling between relevant theory and experiment.

Finally it should be noted that the research conducted under this contract laid the foundations for research on other FEL configurations, namely those of the high energy, zero guide field problems of LANL and LLNL and magnetic crystal FEL γ radiation generation.

In the remainder of this report details of the supported research over the last contract year are presented in Section II, and Section III lists contract supported publications and oral presentations.

II. RECENT PROGRESS

In this section we review the progress made under this contract over the last year.

A. Profile of a Relativistic Electron Beam Propagated through a Linear Wiggler and an Axial Guide Field

Most theoretical analyses of the free-electron laser instability employ highly simplified models in which the electron density is taken to be uniform in space. Noting that a function of the constants of motion of a single electron is a steady-state solution of the Vlasov equation, Davidson and Uhm[1] were the first to construct self-consistent equilibria for electron beams propagated in an axial guide field and a helical wiggler field, and the resulting spatial modulation of the electron density was determined for different choices of the functional dependence of the distribution function on the constants of motion.

In this work, we have examined the experimental situation where the directional flux of electrons (and beam emittance) at the anode is specified and the beam is allowed to propagate through a drift tube immersed in a strong axial guide field and a linear (or planar) wiggler. Using the nonlinear orbits obtained earlier at SAIC/PRI,[2] the distribution function of the electrons at any point along the drift tube is determined from the equation of continuity in phase space and the electron density is then given by an integration over momenta. Unlike the calculation in Ref. 1, the orbits determined earlier[2] permit us to treat the case where there is a resonance between the gyromotion of the electrons and the effective axial periodicity induced by the wiggler. Additionally, the radial dependence of the wiggler field is allowed for.

In Ref. 2 it is argued that in the presence of an axial guide field it is natural to introduce the gyroradius ρ, gyroangle θ, and guiding center coordinates

X and Y. It is then shown that for sufficiently small wiggler fields (measured by $\varepsilon \equiv \delta H/H_0$, δH being the wiggler and H_0 the guide field intensity) the motion of the electrons can be locked onto a single resonance, with the particles strongly influenced by this resonance but mildly so by adjacent harmonics. This resonance condition has the form $\ell\dot{\theta} + k\dot{z} \simeq 0$ for some integer ℓ, where $k = 2\pi/\lambda$, λ is the wiggler wavelength, and $\dot{z}$ is the axial velocity. It is further shown that in this case the motion is nonstochastic, and explicit integration of the equations of motion is then possible. For FEL applications it is imperative to limit the strength of the wiggler so as to avoid stochastic motion.

In the experiment carried out by Roberson et al.[3] at the Naval Research Laboratory, which provided the original motivation for our work, a current of electrons ($\simeq 500$ A) is accelerated through a potential difference of 350 kV ($\gamma \simeq 1.68$) before impinging on an anode of radius $R_0 \simeq 1/2$ cm and entering a drift tube of length 60 cm. In this experiment electric and magnetic self-field effects on particle orbits, which are measured by the dimensionless parameter $(2\gamma\omega_p^2/\Omega_0^2)[1 - (\dot{z}/c)^2] \simeq 1/2$, are nonnegligible. (Here ω_p is the plasma frequency and Ω_0 the guide field cyclotron frequency.) Further, in the experiment the magnetic field was allowed to build to its full value in a transition region preceding the drift tube entrance. The work described in Ref. 2 and herein is idealized in the sense that neither self-field effects nor the effect of a transition region is allowed for.

The electron density at $\underline{r}$ is given by $n(\underline{r}) = \int d^3\underline{p}\, f(\underline{r},\underline{p})$, where f, the electron distribution function at $(\underline{r},\underline{p})$, satisfies the continuity equation in 6-dimensional phase space: $df/dt = 0$. Knowing the beam emittance at the anode and the particle orbits, the indicated integration over momenta can then be performed to determine the density as a function of distance along the drift-tube. A reasonable form for the beam distribution at the anode, located at $z = 0$, is

$$f = \mathscr{C}\Theta(R_0 - R)\delta[(\gamma^2 - 1)m^2c^2 - \underline{p}^2] \exp(-\phi) \quad ,$$

wherein $\mathscr{C}$ is a normalization constant, $\Theta(\cdot)$ is the Heaviside unit step function, R_0 is the anode radius, $R = (x^2 + y^2)^{\frac{1}{2}}$ is the radial distance of the point (x,y) from the axis of the drift-tube, and

$$\phi = \frac{p_x^2 + p_y^2}{\bar{p}_\perp^2} + \left[\frac{p_z - p_b}{\bar{p}_\parallel}\right]^2 \quad ,$$

$\bar{p}_\parallel$ and $\bar{p}_\perp$ being the spread in the parallel and perpendicular momenta of the electrons emerging from the anode, with the parallel momenta being centered about the resonant value $p_b \equiv \ell m|\Omega_0|/k$ (Ref. 2). The Heaviside function in the expression for f indicates that a beam of radius R_0 and of uniform density emerges from the anode. The δ-function indicates that the beam is monoenergetic, with a fixed γ. The experimentally determined spread in the perpendicular speed is roughly given by $(\bar{p}_\perp/mc) \simeq 0.08$-$0.24$; by a simple kinematical argument one finds that $\bar{p}_\parallel \simeq \frac{1}{2}(\bar{p}_\perp^2/p_b)$, whence the spread in parallel speed is determined.

In Fig. 1 the beam density (in arbitrary units) is plotted as a function of the axial distance z from the anode along the drift tube for $\varepsilon = 1/1024$. For the upper curve the observation point at which the density is measured has coordinates $x = 0$, $y = 0.5$ while the lower curve has $x = 0$, $y = 1.0 \times 10^{-2}$. All linear dimensions are given in centimeters and plotted results are accurate to $\lesssim 1\%$. The substantial density modulation evident in the upper curve can be understood by examining the nature of the particle orbits using Fig. 2. In this diagram circle A represents the anode (radius 1.2) and O is the observation point (coordinates $x = 0$, $y = 0.5$). Consider gyro-orbits which enclose circle R, pass through observation point O and have their guiding center on the y-axis (circle R_ℓ for example). Particles in such orbits necessarily move beyond the anode radius during part of their trajectory. Since the beam has little spread in parallel momentum by far the greatest number of particles have gyroradii of 0.453, that of particles exactly at resonance ($p_z = p_b = \ell m|\Omega_0|/k$). Circles R_ℓ and R_u are gyro-orbits that bound this most probable value, and are populated with 1×10^{-4} of the number of particles at resonance. As we move forward in space from the anode, the particles in the relevant orbits (denoted by the shaded regions) move outside A and the density at O falls. For $\ell = 2$, the resonance condition $\ell\dot{\theta} + k\dot{z} \simeq 0$ implies that in one wiggler wavelength (3 cm) the particles complete about half of their gyro-orbit and the density should be minimum. Over a distance of two wiggler wavelengths the particles return to their original locations (in the limit where all parallel momenta are identical) and the density is again at its peak.

Because a small spread in parallel momenta actually exists, particles completing their orbits return to their original positions at slightly different times, producing a smaller modulation of density evident in the shorter wavelength oscillations in the upper curve of Fig. 1 and the latter part of the lower curve. (The initial oscillations of density in the lower curve are numerical noise.)

Of course, there are other regions besides the shaded area in Fig. 2 which contribute to the plotted density modulations. We have simplified our discussion and diagram to keep the argument clear. By recalling, however, that the only significant gyroradii are approximately 0.45 and that the observation point is 0, it is easy to see that the only particles contributing to the density modulation lie in an appropriately expanded shaded region symmetrically placed about the y-axis. For instance, since the radius of circle L in Fig. 2 is 0.85, practically no particle with a guiding center lying on the y-axis to the left of 0 whose orbit passes through 0 moves out of A. Such a particle, therefore, does not contribute to the observed density depletion.

The wiggler acts to alter the speed of the particles as they move along the drift tube. By increasing the amplitude of the wiggler field an enhancement of the shorter-wavelength modulation seen in Fig. 1 is expected. This is clearly evident in Figs. 3 and 4 in which $\varepsilon = 1/128$ and $\varepsilon = 1/64$ respectively. It is this short-wavelength modulation that is apparently discussed in Ref. 1, for in that work it is assumed there is no spread in the parallel momenta of the electrons.

We next define the parallel temperature by

$$nT_z \equiv \int d^3\underline{p}\ f(\underline{r},\underline{p})\gamma m\left|\frac{p_z}{\gamma m} - V_z(\underline{r})\right|^2$$

where the mean parallel velocity is given by

$$nV_z = \int d^3\underline{p}\ f(\underline{r},\underline{p})\frac{p_z}{\gamma m} \quad .$$

The quantity T_z is a measure of the spread in parallel velocities in the beam frame. In order that the electromagnetic radiation emitted by the electrons be as coherent as possible, T_z must be small. The normalized parallel temperature $T \equiv (ck/\ell|\Omega_0|)^2(\gamma T_z/mc^2)$ as a function of z for $\varepsilon = 1/128$ and $y = 0.5$ is shown in Fig. 5. The initial rise in T can be understood as the consequence of an effective spread in parallel momenta as particles with $p_z \simeq p_b$ orbit out of the anode radius and vacate observation point 0. The subsequent increase in T is due to asynchronism of particle motion. Note that, although T increases by almost two orders of magnitude it is still not very large, about 10 keV at $z \simeq 24$ cm.

The effects of increasing the beam energy on the density modulation are shown in Fig. 6. Here $\varepsilon = 1/128$, $y = 0.5$ and the $\ell = 3$ harmonic is resonant ($\gamma = 2.62$). Note the larger density depletion than in the $\ell = 2$ case. This is readily understood since the most probable gyroradius is now 0.65 and a greater fraction of electrons have trajectories which take them beyond the anode radius.

In conclusion, this work indicates that significant density modulation can be expected from the axial guide field, the wiggler, and the spread in parallel momenta. This may be expected to greatly limit laser gain, particularly in cases where a typical gyroradius is not appreciably smaller than the anode dimension.

B. Influence of Finite Radial Geometry on Coherent Radiation Generation by a Relativistic Electron Beam in a Longitudinal Magnetic Wiggler

The influence of finite radial geometry on the longitudinal wiggler free electron laser instability has been investigated[3] for TE mode perturbations about a uniform density electron beam with radius $\hat{R}_b$ (see Fig. 1). The equilibrium and stability analysis is carried out for a think tenuous electron beam propagating down the axis of a multiple-mirror (undulator) magnetic field $\underset{\sim}{B}_0(\underset{\sim}{x}) \simeq B_0[1 + (\delta B/B_0)\sin k_0 z]\hat{\underset{\sim}{e}}_z$, where $\lambda_0 = 2\pi/k_0$ = const. is the wiggler wavelength. It is assumed that $k_0^2\hat{R}_b^2 \ll 1$, and that perturbations are about the self-consistent Vlasov equilibrium $f_b^0(\underset{\sim}{x},\underset{\sim}{p}) = (\hat{n}_b/\pi)\delta(p_\perp^2 - 2\gamma_b m\omega_b P_\theta - 2\gamma_b m\hat{T}_{\perp b}) \times \delta(p_z - \gamma_b m V_b)$, where $p_\perp^2 = p_r^2 + p_\theta^2$, P_θ is the canonical angular momentum, and $\hat{n}_b$, γ_b, ω_b, $\hat{T}_{\perp b}$ and V_b are positive constants. For $\delta B/B_0 \ll 1$ and slow beam rotation ($\omega_b \ll \omega_{cb} = eB_0/\gamma_b mc$), the equilibrium density is uniform ($\hat{n}_b$) out to the beam radius $\hat{R}_b = (2\hat{T}_{\perp b}/\gamma_b m\omega_b\omega_{cb})^{\frac{1}{2}}$. Detailed free electron laser stability properties are investigated for the case where the amplifying radiation field has TE-mode polarization with perturbed field components $(\delta\hat{E}_\theta, \delta\hat{B}_r, \delta\hat{B}_z)$. The matrix dispersion equation[3] is analyzed in the diagonal approximation, and it is shown that the positioning of the beam radius $(\hat{R}_b)$ relative to the conducting wall radius (R_c) can have a large influence on the growth rate and detailed stability properties. Analytic and numerical studies show that the growth rate increases as $\hat{R}_b/R_c$ is increased.[3]

C. Compton and Raman Free Electron Laser Stability Properties for a Cold Electron Beam Propagating through a Helical Magnetic Wiggler

Under the auspices of the present contract we have given an extensive characterization[4] of the range of validity of the Compton and Raman approximations to the exact free electron laser dispersion relation for a cold, relativistic electron beam propagating through a constant-amplitude helical wiggler magnetic field $\underset{\sim}{B}_w = -\hat{B}\cos k_0 z\hat{\underset{\sim}{e}}_x - \hat{B}\sin k_0 z\hat{e}_y$. Here, $\lambda_0 = 2\pi/k_0$ is the wiggler wavelength, $\hat{B}$ the wiggler amplitude (assumed constant), and the electron beam is treated as infinite in transverse extent. For example, a detailed numerical analysis shows that the Compton approximation ($\delta\phi \simeq 0$) gives a valid estimate, to within ten percent, of the maximum growth rate of the upshifted emission peak for system parameters satisfying

$$\frac{\omega_p c k_0}{\omega_c^2} < \frac{\gamma_b^3}{25}\frac{(1+\beta_b)}{\beta_b} \quad . \tag{1}$$

Here, $\omega_p^2 = 4\pi\hat{n}_b e^2/\bar{\gamma}m$ is the relativistic plasma frequency-squared, $\omega_c = e\hat{B}/\bar{\gamma}mc$ is the relativistic cyclotron frequency, $\gamma_b = (1-\beta_b^2)^{-\frac{1}{2}}$ is the relativistic mass factor, $\beta_b c = p_0/\bar{\gamma}m$ is the axial beam velocity, $\bar{\gamma}$ is defined by $\bar{\gamma} \equiv (1 + p_0^2 m^2 c + e^2\hat{B}^2/m^2c^4k_0^2)^{\frac{1}{2}}$, and $G_0(p_z) = \delta(p_z - p_0)$ is the equilibrium axial momentum distribution of the beam electrons.

D. <u>Influence of Beam Quality on Free Electron Laser Growth Rate for an Intense Electron Beam Propagating through a Helical Magnetic Wiggler</u>

We have made use of the fully kinetic dispersion relation derived by Davidson and Uhm[5] to investigate the influence of beam quality on FEL growth rate for a relativistic electron beam propagating through a helical wiggler field $\underset{\sim}{B}_w = -\hat{B}\cos k_0 z\hat{\underset{\sim}{e}}_x - \hat{B}\sin k_0 z\hat{\underset{\sim}{e}}_y$. Assuming a sufficiently tenuous beam that the Compton-regime approximation is valid ($\delta\phi \simeq 0$), and assuming weak resonant instability with small temporal growth rate γ_k satisfying $|\gamma_k/\omega_k| \ll 1$ and $|\gamma_k/k\Delta v_z| \ll 1$, it is found that the growth rate can be approximated by

$$\gamma_k = \frac{\pi}{4}\frac{\hat{\omega}_c^2}{c^2k_0^2}\,\omega_p^2\bar{\gamma}^{-3}m^2c^2\,\frac{1}{\left[1+\left(\frac{eB/mc}{ck_0}\right)^2\right]}\,\frac{k}{\omega_k|k|}\left[\gamma\frac{\partial G_0}{\partial p_z}\right]_{v_z=\frac{\omega_k}{k}} \tag{2}$$

for small fractional momentum spread in the beam electrons ($\Delta p_z/p_0 \ll 1$). Here, $G_0(p_z)$ is the equilibrium distribution, $\hat{\omega}_c = e\hat{B}/\bar{\gamma}mc$ is the cyclotron frequency,

$\hat{\omega}_p^2 = 4\pi\hat{n}_b e^2/\bar{\gamma}m$ is the plasma frequency-squared, and $\bar{\gamma}mc^2 = (m^2c^4 + c^2p_0^2 + e^2\hat{B}^2/k_0^2)^{\frac{1}{2}}$ is the average energy.

For waves excited with positive phase velocity $\omega_k/k > 0$, it follows from Eq. (2) that $\gamma_k \gtrless 0$ accordingly as $[\gamma\partial G_0/\partial p_z]_{v_z=\omega_k/k} \gtrless 0$. That is, waves with phase velocity in the region of positive momentum slope of $G_0(p_z)$ are amplified, corresponding to instability with $\gamma_k > 0$. As a specific example, we have investigated detailed growth rate properties for the case where the beam distribution is Gaussian in p_z with

$$G_0(p_z) = \left(\frac{2}{\pi}\right)^{\frac{1}{2}} \frac{1}{\Delta p_z} \exp\left[-\frac{2(p_z - p_0)^2}{\Delta p_z^2}\right] \quad . \tag{3}$$

Typical results are shown in Figs. 8 and 9 where γ_k/k_0c is plotted versus k/k_0 for fixed values of $\hat{\omega}_c/ck_0$ and $\bar{\gamma}$, and different choices of the dimensionless parameters $\Delta p_z/p_0$ and $\omega_p^2/c^2k_0^2$. Note from Figs. 8 and 9 that the instability bandwidth $\Delta k/k_0$ increases by almost an order-of-magnitude as $\Delta p_z/p_0$ is increased from 2.8×10^{-3} to 2×10^{-2}. Also, the maximum growth rate increases substantially as $\omega_p^2/c^2k_0^2$ is increased from 3.62×10^{-5} to 1.28×10^{-2}. [See also Eq. (2).]

III. CONTRACT SUPPORTED FEL RESEARCH PUBLICATIONS/ORAL PRESENTATIONS

"Profile of a Relativistic Electron Beam Propagated through a Linear Wiggler and an Axial Guide Field," B. Hafizi, G. L. Francis, and R. E. Aamodt, SAIC report # SAIC-84-1428/PRI-86, to be published.

"Long-Time Quasilinear Evolution of the Free Electron Laser Instability for a Relativistic Electron Beam Propagating through a Helical Magnetic Wiggler," R. C. Davidson and Y. Z. Yin, submitted for publication (1984).

Influence of Intense Equilibrium Self-Fields on the Spontaneous Emission from a Test Electron in a Realtivistic Nonneutral Electron Beam," Ronald C. Davidson and Wayne A. McMullin, Phys. Fluids 27, 1268 (1984).

"Influence of Finite Radial Geometry on Coherent Radiation Generation by a Relativistic Electron Beam in a Longitudinal Magnetic Wiggler," Ronald C. Davidson and Yuan-Zhao Yin, Phys. A30, 3078 (1984).

"Compton and Raman Free Electron Laser Stability Properties for a Cold Electron Beam Propagating through a Helical Magnetic Wiggler," John A. Davies, Ronald C. Davidson, and George L. Johnston, J. Plasma Phys. 32, in press (1985).

"Cross-Field Free Electron Laser Instability for a Tenuous Electron Beam," Ronald C. Davidson, Wayne A. McMullin, and Kang Tsang, Phys. Fluids 27, 233 (1984).

"Nonlinear Orbits in Free-Electron Lasers with a Linear Magnetic Wiggler and a Strong Axial Magnetic Guide Field," B. Hafizi and R. E. Aamodt, Phys. Rev. A29 2656 (1984).

"Nonlinear Traveling-Wave Equilibria for Free-Electron-Laser Applications," Barton Lane and Ronald C. Davidson, Phys. Rev. A27, 2008 (1983).

"Effects of Self-Electric and Self-Magnetic Fields on the Raman FEL Instability," R. C. Davidson, G. L. Johnston, and W. A. McMullin, Bull. APS 28, 1061 (1983).

"Studies of a Tenuous Beam Cross-Field Free-Electron, R. D. Estes, W. A. McMullin, R. C. Davidson, K. Tsang, and A. T. Drobot, Bull. APS 28, 1142 (1983).

"Nonlinear Electron Orbits in Free Electron Lasers with Axial Guide Field," B. Hafizi and R. E. Aamodt, Bull. APS 28, 1062 (1983).

"Proposal for Continued Support of Research on Conversion Efficiencies of Charged Particle Beam Driven Free Electron Lasers," SAI Proposal 1-254-71-840-03, 10 June 1983.

"Intense Free Electron Laser Harmonic Generation in a Longitudinal Magnetic Wiggler," Ronald C. Davidson and Wayne A. McMullin, Phys. Fluids 26, 840 (1983).

"Free Electron Laser Instability for a Relativistic Solid Electron Beam in a Helical Wiggler Field," Han S. Uhm and Ronald C. Davidson, Phys. Fluids 26, 288 (1983).

"Electron Orbits in a Free-Electron Laser with a Longitudinal Magnetic Wiggler," R. E. Aamodt, Phys. Rev. A28, 2895 (1983).

"Nonlinear Bernstein-Greene-Kruskal Wave Equilibria Subject to Global Energy and Momentum Conservation Constraints," R. C. Davidson and K. T. Tsang, J. Appl. Phys. 54, 6284 (1983).

"Low Gain Free Electron Laser near Cyclotron Resonance," Wayne A. McMullin and Ronald C. Davidson, Phys. Rev. A25, 3130 (1982).

"Stability Properties of an Intense Relativistic Non-Neutral Electron Ring in a Modified Betatron Accelerator," Ronald C. Davidson and Han S. Uhm, Phys. Fluids 25, 2089 (1982).

"Relativistic Electron Beam Equilibria with Non-Circular Cross Section," Ronald C. Davidson, Particle Accelerators 12, 55 (1982).

"Helically Distorted Relativistic Electron Beam Equilibria for Free Electron Laser Applications," Ronald C. Davidson and Han S. Uhm, J. Appl. Phys. 53 2910 (1982).

"Higher Harmonic Emission by a Relativistic Electron Beam in a Longitudinal Magnetic Wiggler," Ronald C. Davidson and Wayne A. McMullin, Phys. Rev. A26, 1997 (1982).

"Proposal for Continued Support of Research on Conversion Efficiencies of Charged Particle Beam Driven Free Electron Lasers, SAI Proposal 1-254-71-830-03, 11 May 1982.

"Stochastic Particle Instability for Electron Motion in Combined Helical Wiggler, Radiation, and Longitudinal Wave Fields," Ronald C. Davidson and Wayne A. McMullin, Phys. Rev. A26, 410 (1982).

"Free Electron Laser Instability for a Relativistic Annular Electron Beam in a Helical Wiggler Field," Han S. Uhm and Ronald C. Davidson, Phys. Fluids 24, 2348 (1981).

"Theory of Free Electron Laser Instability in a Relativistic Annular Electron Beam," Han S. Uhm and R. C. Davidson, Phys. Fluids 24, 1541 (1981).

"Proposal for Continued Support of Research on Conversion Efficiencies of Charged Particle Beam Driven Free Electron Lasers," SAI Proposal 1-254-71-820-01, 20 February 1981.

"Self-Consistent Vlasov Description of the Free Electron Laser Instability Ronald C. Davidson and Han S. Uhm, Phys. Fluids 23, 2076 (1980).

"Low-Frequency Flute Instabilities in Intense Nonneutral Electron and Ion Beams," Han S. Uhm and Ronald C. Davidson, Phys. Fluids 23, 1586 (1980).

"Proposal for Support of Research on Conversion Efficiencies of Charged Particle Beam Driven Free Electron Lasers," SAI Proposal 1-254-71-810-03, 14 May 1980.

"Semiannual Status Report of ONR Contract No. N00014-79-C-0555 with Science Applications, Inc., titled: Conversion Efficiencies of Charged Particle Beam Driven Free Electron Lasers," December 1979.

"Influence of Finite Radial Geometry on the Free Electron Laser Instability R. C. Davidson, H. S. Uhm, and R. Aamodt, Bull. APS 24, 1066 (1979).

Oral Presentation to NRL, Washington, by Richard E. Aamodt, May 1982.

REFERENCES

1. R. C. Davidson and H. S. Uhm, J. Appl. Phys. 53, 2910 (1982).

2. B. Hafizi and R. E. Aamodt, Phys. Rev. A29, 2656 (1984).

3. "Influence of Finite Radial Geometry on Coherent Radiation Generation by a Relativistic Electron Beam in a Longitudinal Magnetic Wiggler," R. C. Davidson and Y. Z. Yin, submitted for publication (1984).

4. "Compton and Raman Free Electron Laser Stability Properties for a Cold Electron Beam Propagating through a Helical Magnetic Wiggler," J. A. Davies, R. C. Davidson and G. L. Johnston, submitted for publication (1984).

5. R. C. Davidson and H. S. Uhm, Phys. Fluids 23, 2076 (1980).

FIGURE CAPTIONS

Fig. 1. Normalized density D as a function of the distance z (in cm) measured from the anode along the drift tube. Wiggler wavelength $2\pi/k = 3$ cm, $\gamma = 1.68$, guide field $H_0 = 2.2$ kOe, $\varepsilon \equiv \delta H/H_0 = 1/1024$, resonance harmonic number $\ell = 2$, radius of anode $R_0 = 1.2$ cm. Observation point for lower curve has coordinates $(x,y) = (0,10^{-2})$ cm, for upper curve $(x,y) = (0,0.5)$ cm.

Fig. 2. Relationship between anode and typical gyro-orbits at observation point O with coordinates $(x,y) = (0,0.5)$ cm.

Fig. 3. Same parameters as Fig. 1, but with $\varepsilon = 1/128$.

Fig. 4. Same parameters as Fig. 1, but with $\varepsilon = 1/64$.

Fig. 5. Normalized parallel temperature $T \equiv (ck/\ell|\Omega_0|)^2(\gamma T_z/mc^2)$ as a function of distance along the drift tube. Here $\varepsilon = 1/128$ and the observation point has coordinates (0,0.5) cm.

Fig. 6. Same parameters as Fig. 1, but with $\gamma = 2.26$, $\ell = 3$, $\varepsilon = 1/128$. The observation point for this curve has coordinates $(x,y) = (0,0.5)$ cm.

Fig. 7. Geometry and coordinate system for longitudinal wiggler free electron laser.

Fig. 8. Plot of normalized growth rate γ_k/k_0c versus k/k_0 [Eq. (2)] for helical wiggler FEL with $e\hat{B}/mc^2k_0 = 0.718$, $\omega_p^2/c^2k_0^2 = 3.62 \times 10^{-5}$ $\bar{\gamma} = 47.1$, $p_0 = 1.286 \times 10^{-15}$ g-sem/sec, and $\Delta p_z/p_0 = 2.8 \times 10^{-3}$

Fig. 9. Plot of normalized growth rate γ_k/k_0c versus k/k_0 [Eq. (2)] for helical wiggler FEL with $e\hat{B}/mc^2k_0 = 0.718$, $\omega_p^2/c^2k_0^2 = 1.28 \times 10^{-2}$, $\bar{\gamma} = 47.1$, $p_0 = 1.286 \times 10^{-15}$ g-cm/sec, and $\Delta p_z/p_0 = 2 \times 10^{-2}$.

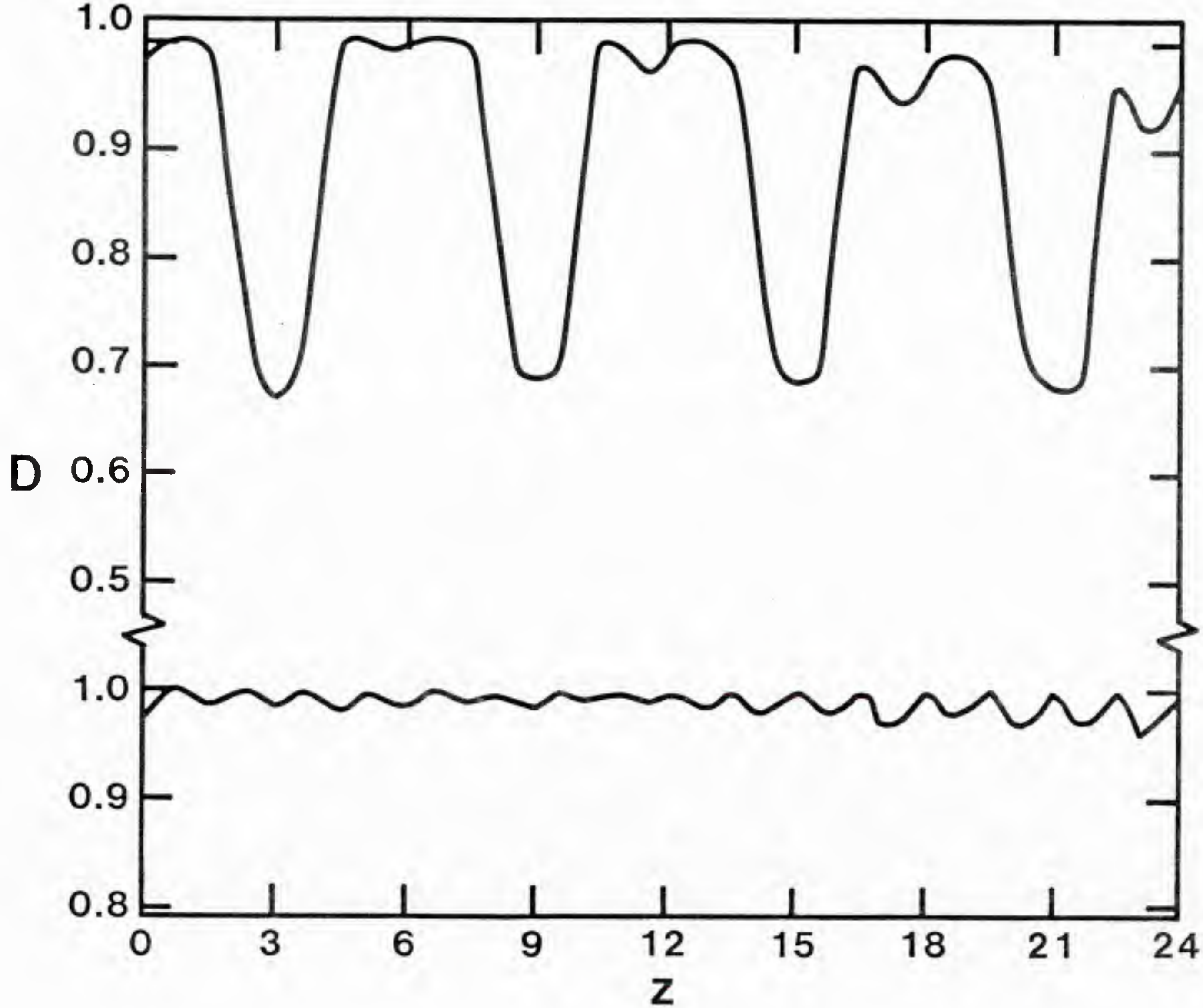

Fig. 1

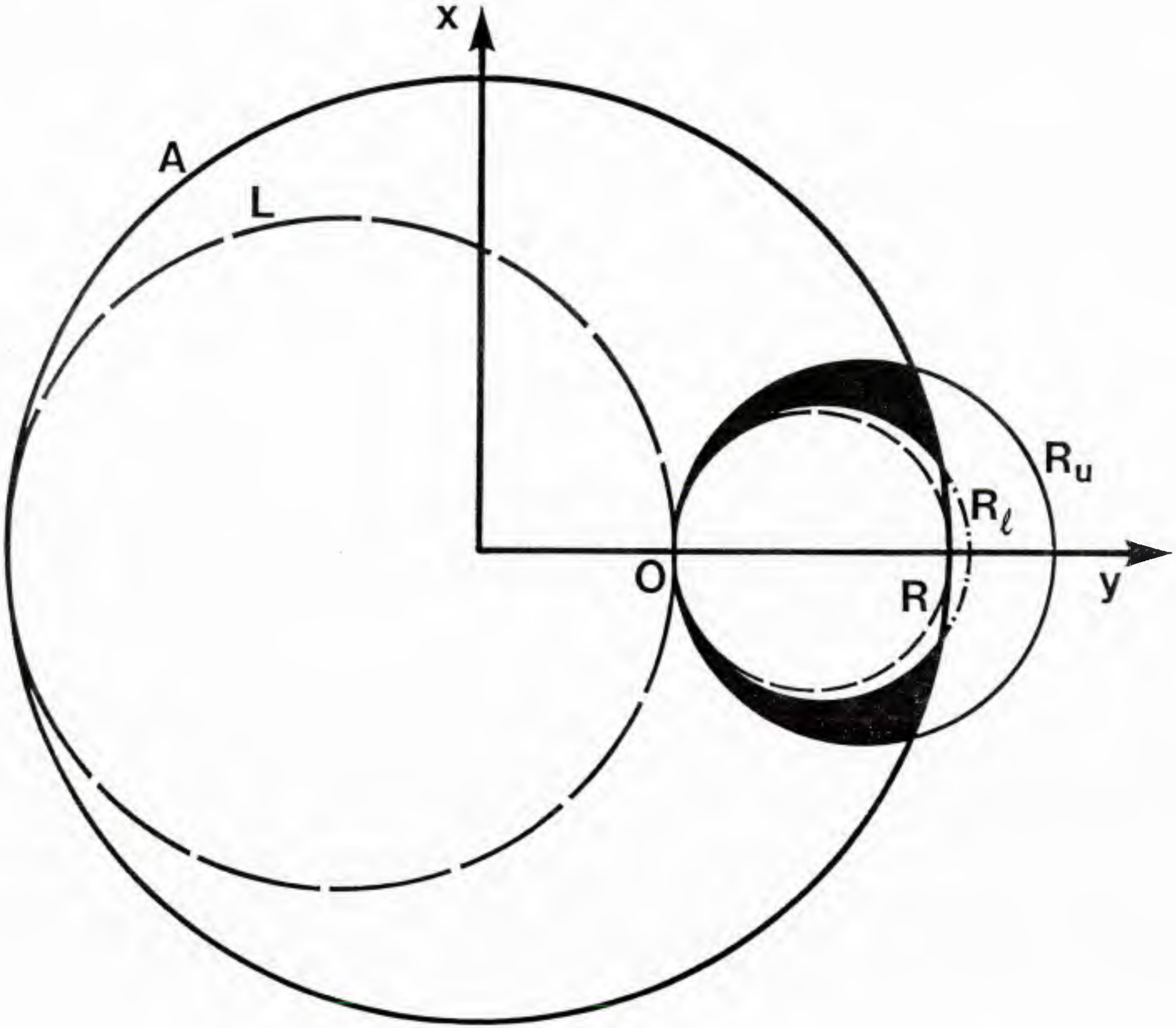

Fig. 2

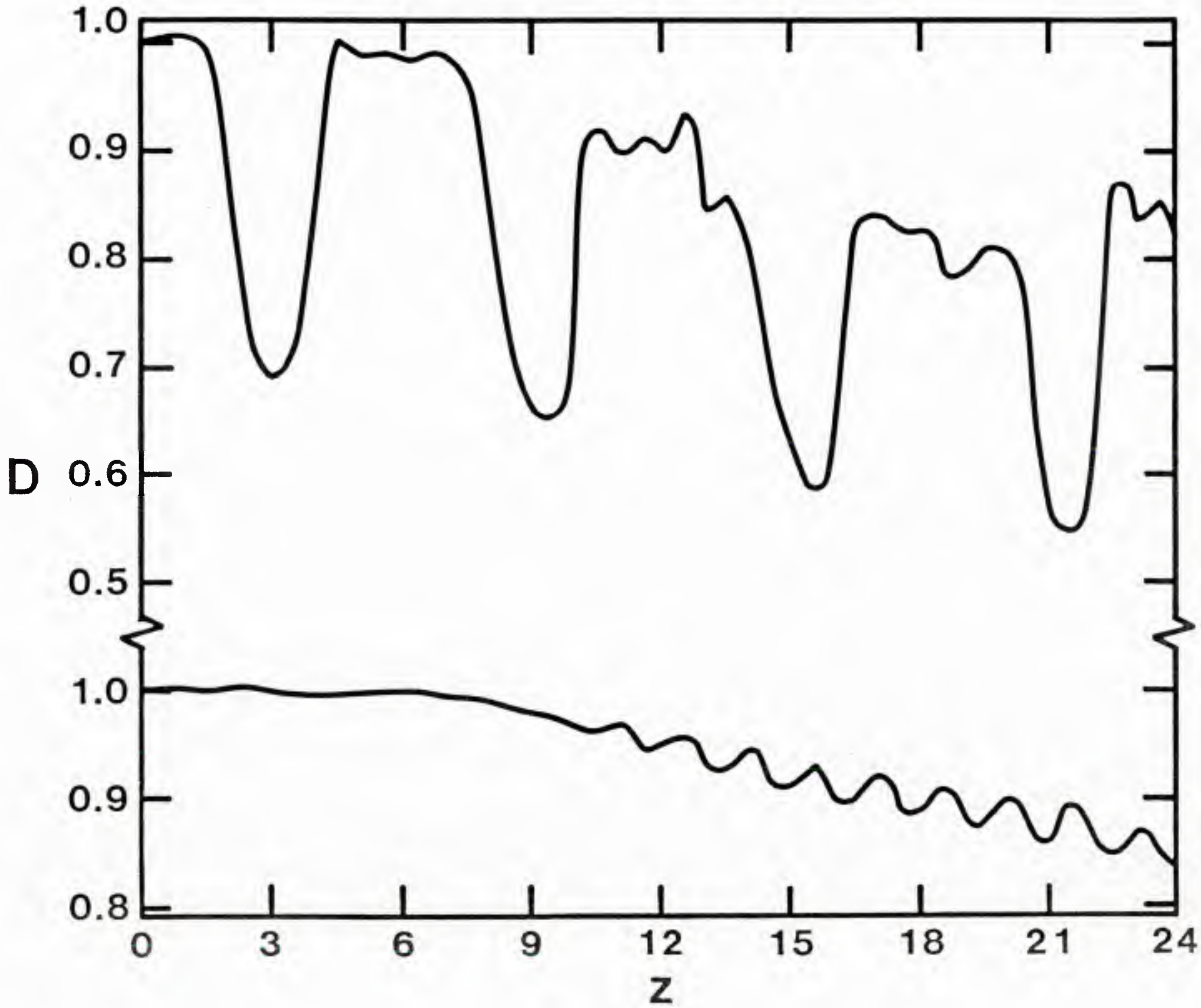

Fig. 3

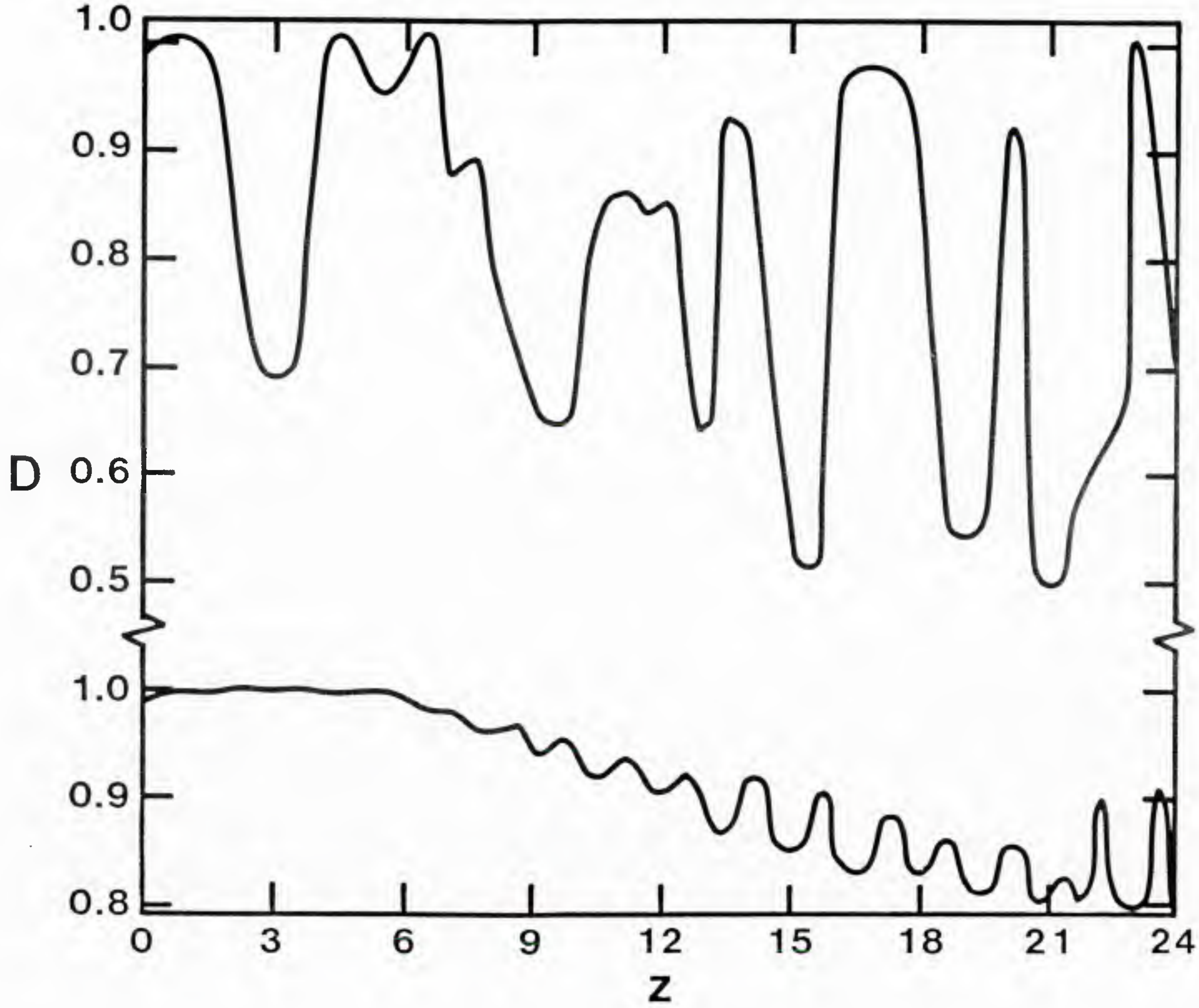

Fig. 4

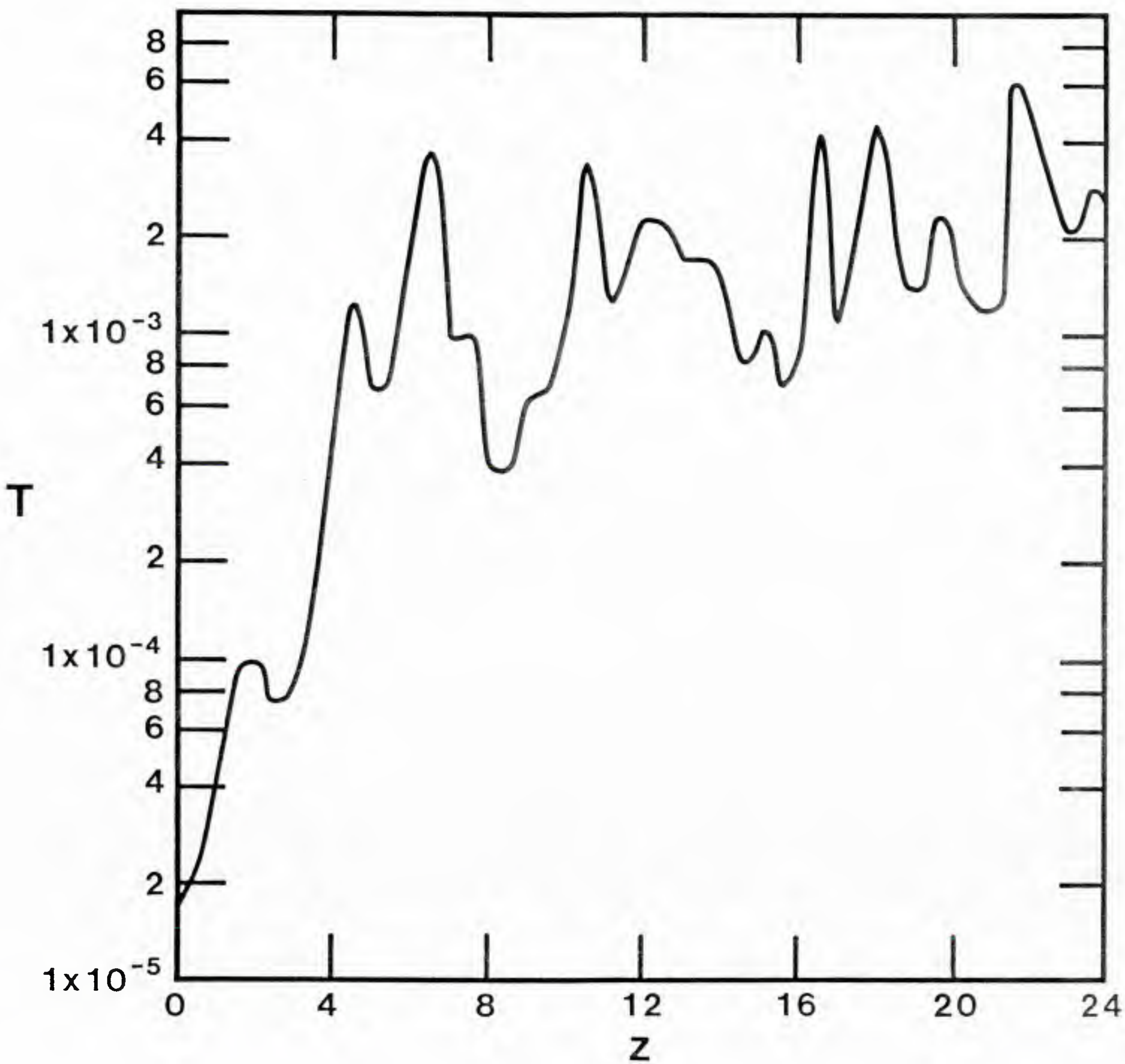

Fig. 5

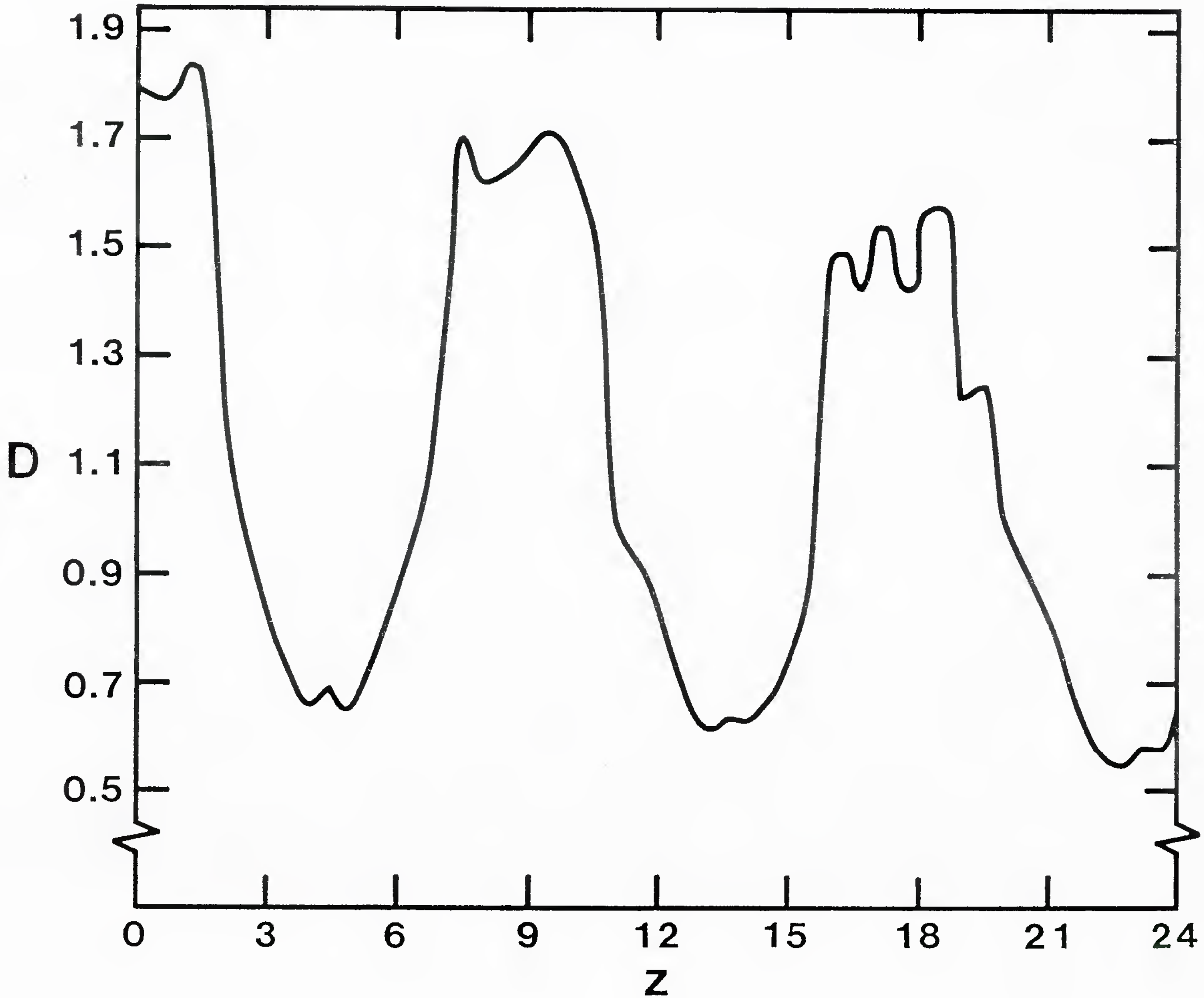

Fig. 6

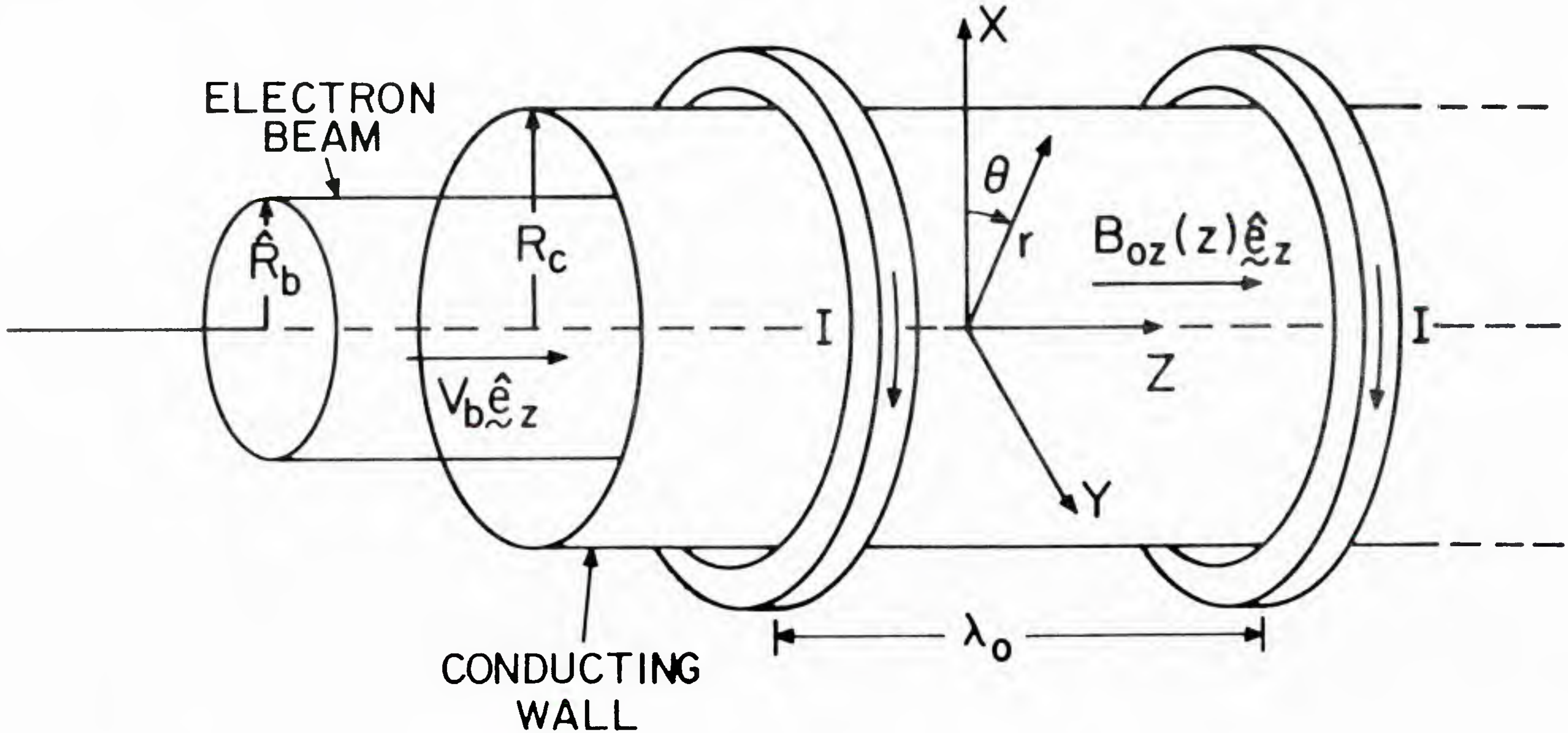
ELECTRON
BEAM
$\hat{R}_b$
R_c
$V_b \hat{e}_z$
CONDUCTING
WALL
X
θ
r
Y
Z
$B_{oz}(z)\hat{e}_z$
I
I
λ_o

Fig. 7

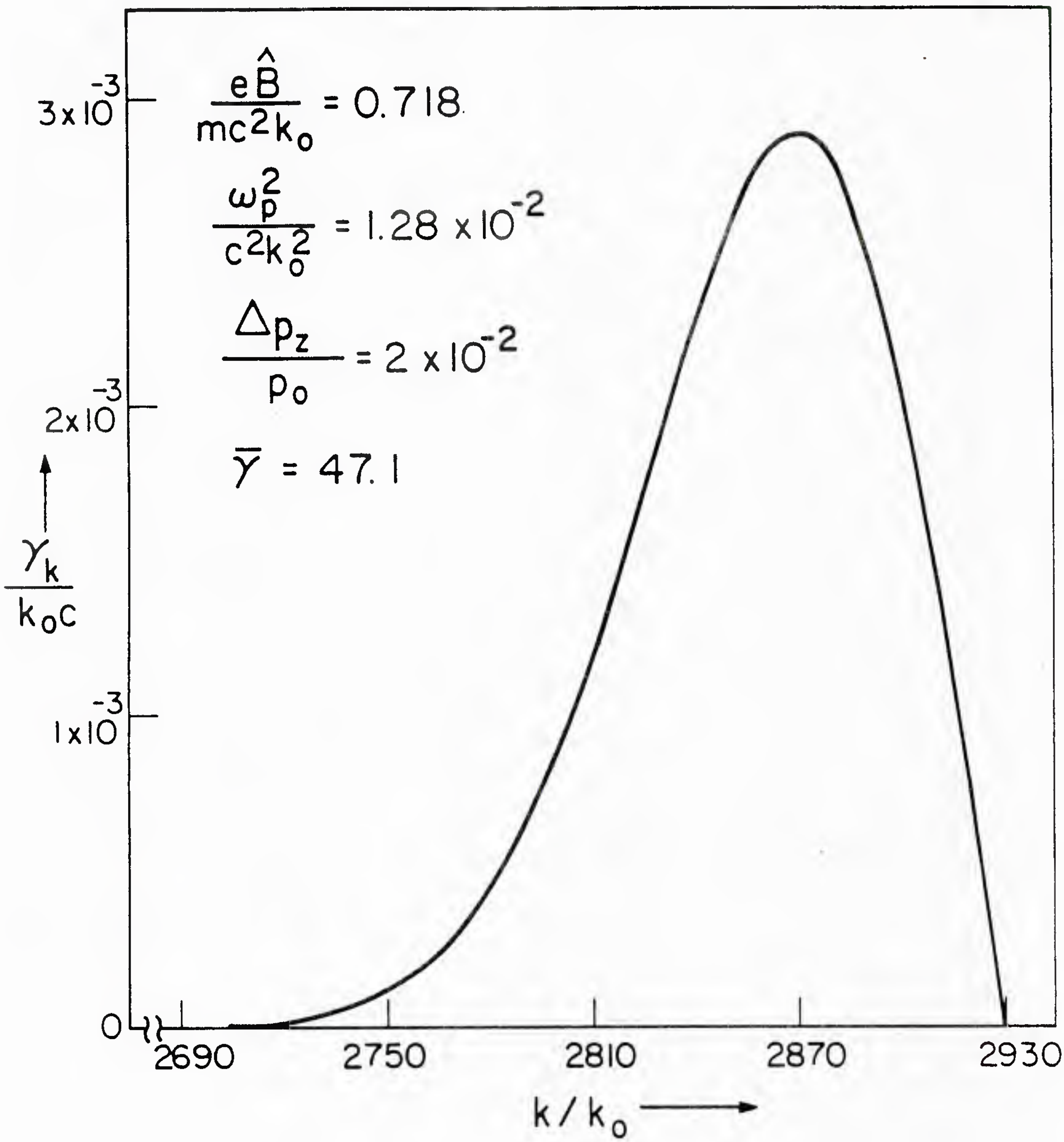

$\frac{e\hat{B}}{mc^2k_o} = 0.718$
$\frac{\omega_p^2}{c^2k_o^2} = 1.28 \times 10^{-2}$
$\frac{\Delta p_z}{p_o} = 2 \times 10^{-2}$
$\bar{\gamma} = 47.1$
3×10^{-3}
2×10^{-3}
1×10^{-3}
0
$\frac{\gamma_k}{k_o c}$
2690
2750
2810
2870
2930
k/k_o

Fig. 8

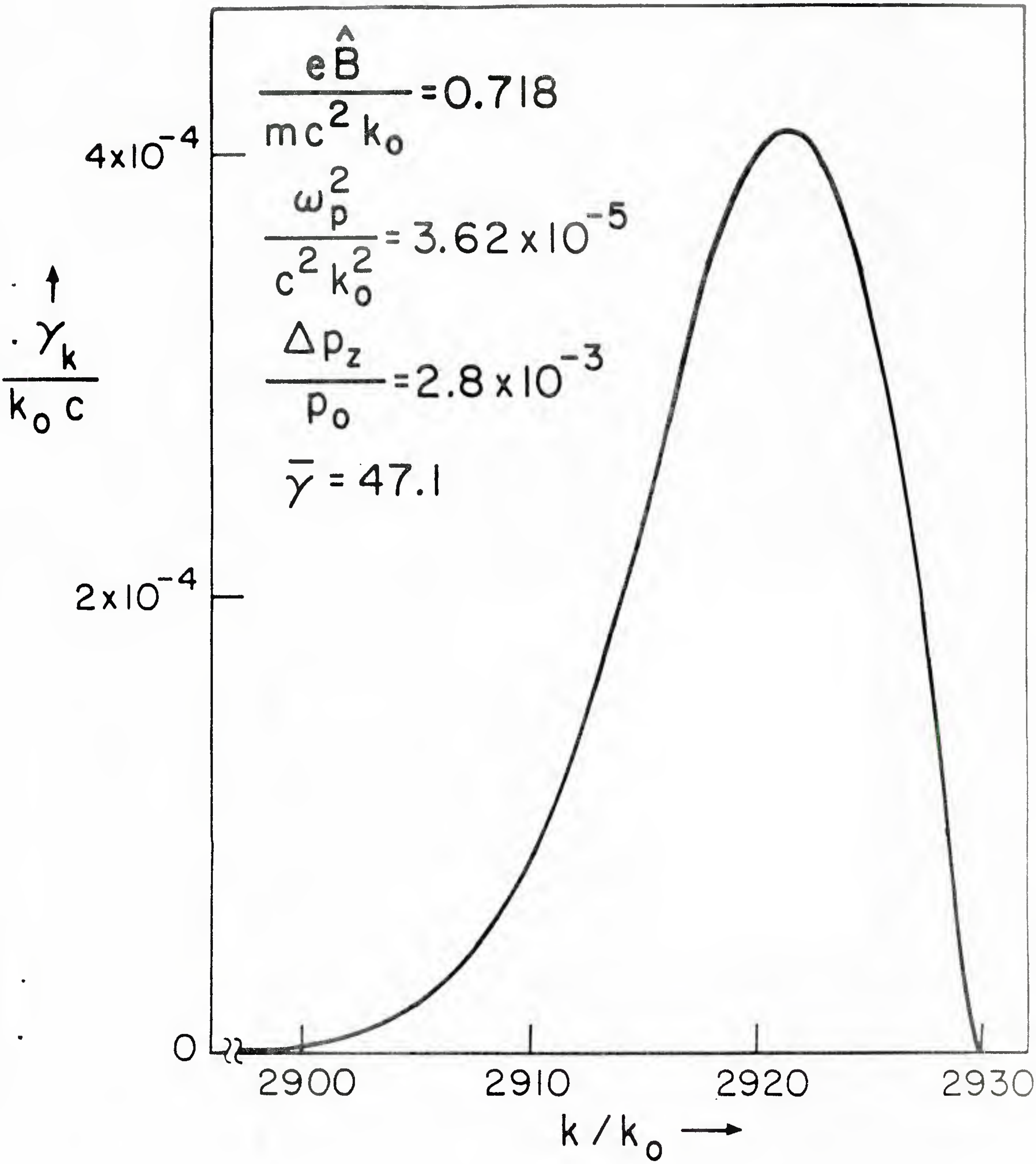

$\frac{e\hat{B}}{mc^2 k_0} = 0.718$
$\frac{\omega_p^2}{c^2 k_0^2} = 3.62 \times 10^{-5}$
$\frac{\Delta p_z}{p_0} = 2.8 \times 10^{-3}$
$\bar{\gamma} = 47.1$
4×10^{-4}
2×10^{-4}
0
$\frac{\gamma_k}{k_0 c}$
2900
2910
2920
2930
k/k_0

Fig. 9